

Technical Paper

Deflection hardening behavior and elastic modulus of one-part hybrid fiber-reinforced geopolymer composites

Yazan Alrefaei, and Jian-Guo Dai*

(Received July 24, 2019; Revised December 22, 2019; Accepted December 23, 2019; Published December 31, 2019)

Abstract: This paper reports for the first time the experimentally tested elastic modulus values of the fiber-reinforced geopolymer composites (FRGCs). Further, the deflection hardening behavior and sand addition effect on the ambient-cured one-part steel-polyethylene FRGCs are also reported wherein the total fiber volume fraction used was 2%.

It was found that although the cylinders' compressive strength of the blended-based FRGCs was relatively higher than that of the slag-based FRGCs, the latter showed a relatively larger elastic modulus in comparison with the former. The addition of fiber increased the elastic modulus of the geopolymer composites relative to the none-fibrous composites at which the elastic modulus improvement was related to the steel (ST) volume. Further, all the FRGCs exhibited a deflection hardening behavior which was directly related to the polyethylene (PE) volume included in the composite. Generally, the slag-based FRGCs showed better flexural behavior (i.e. modulus of rupture, deflection capacity, and multiple-cracking behavior) in reference to the blended-based FRGCs. The sand addition (i.e. small size like 212 μm with low content such as 30% by mass) was found to improve both flexural cracking and ultimate strengths without affecting the deflection capacity nor the cracking behavior. This could be due to the better volume stability and lower shrinkage of the geopolymer matrix after sand addition.

Keywords: Alkali-activated materials; Fly ash; Slag; Strain hardening; Multiple cracking; Elastic modulus.

1. Introduction

Fiber reinforced cementitious composites (FRC-Cs) have been studied extensively in the past decades and yet are still being researched and developed up to date. FRCC is the general terminology used to describe all fibrous cementitious composites in which a subgroup named ductile fiber-reinforced cementitious composites (DFRCC) was developed later on. DFRCC terminology was used to describe the composites that exhibit a multiple-cracking behavior in flexure only. A special class of DFRCCs termed as High-Performance fiber reinforced cementitious composites (HPFRCC) was formed to represent the composites that attain strain hardening and multiple cracking in both tension and flexure. Such classification was introduced by the DFRCC committee in the Japan Concrete Institute (JCI) [1].

Yazan Alrefaei is a Graduate Student of Civil and Environmental Engineering, The Hong Kong Polytechnic University, Hong Kong.

Corresponding author Jian-Guo Dai is a Professor of Civil and Environmental Engineering, The Hong Kong Polytechnic University, Hong Kong.

One of the commonly known examples of HPFRCCs is the engineered cementitious composites (ECC) that include about 2% fiber content (by volume) and can attain a strain capacity of up to 8% [2, 3]. Thanks to such high ductility and strength, the ECCs are proposed for several structural implementations [4, 5]. However, in order to manufacture such high-ductile ECCs, a relatively large volume of cement should be used, up to 2-3 times that required for concrete production [6]. Accordingly, the sustainability and eco-friendliness performances of ECCs will be concerning as the cement production is responsible for 5-7% of the total CO₂ emissions worldwide [7]. Therefore, the researchers headed to implement the idea of clinker-free cement-less geopolymer binders in FRCCs to develop a new class of green materials called "Fiber Reinforced Geopolymer Composites" (FRGCs) and "Engineered Geopolymer Composites" (EGCs).

Despite the fact that the FRGCs' research area is reasonably new [8], many studies were conducted on the tensile behavior of FRGCs reinforced with several types of either mono [9-15] or hybrid [16-19]

fibers (i.e. basalt, carbon, cotton, glass, polypropylene (PP), polyvinyl alcohol (PVA), polyethylene (PE) and steel) and synthesized using different precursors (i.e. fly ash-based, slag-based and blended-based). Further, limited studies also investigated the flexural behavior of the FRGCs whether reinforced with mono-fibers [8, 18, 20-22] or hybrid-fibers [17, 19, 23, 24]. On the other hand, the elastic modulus (E) of the FRGCs was barely tested in experiments according to previous literature [17]; yet, part of the research reported the theoretical E calculated based on the matrix fracture properties [12, 16, 21, 25, 26].

Generally, the production of geopolymer binders can follow two terminologies either “one-part” or “two-part” [27-29]. The two-part terminology requires the application of solution type activators to activate the aluminosilicate precursors, while the one-part or “just add water” terminology implements the use of solid activators that are pre-mixed with the precursors before the addition of water. Due to the relatively high corrosiveness and hostility of the alkali activator solutions [30], it is predicted that the implementation of two-part geopolymer binders will prosper in the precast concrete industry where the casting environments in factories are more controllable. On the other hand, the one-part geopolymer binders will provide an easy toolkit alternative to ordinary Portland cement (OPC) for in-situ applications; yet such methodology is still under research. According to previous research [27, 31], the commercial anhydrous sodium metasilicate is the most commonly used and efficient solid activator in the industry of one-part geopolymer binders.

Overall, the bulk of the studies mentioned in the literature followed the terminology of two-part geopolymer, while limited studies dealt with the one-part FRGCs [16, 25, 32]. Further, the research related to ambient-cured FRGC focused on the blended-based geopolymer [17, 18, 20, 23, 33] (i.e. fly ash-slag combinations with different ratios), however finite papers investigated the slag-based geopolymer behavior when incorporated with fibers [32]. Additionally, some studies focused on the fiber hybridization concept [17, 22-24, 34] including steel, PP and PVA fibers, yet no study was conducted on the hybrid combination of straight steel fiber and PE. Hence, there is a short in the research related to the flexural behavior and elastic modulus of FRGCs, especially when incorporated with hybrid-fibers and one-part geopolymer concepts.

The aim of this study is to better understand the effect of combining the concepts of hybrid-fibers and one-part geopolymer on the mechanical behavior of FRGCs to permit the structural implementations of FRGCs as green repairing materials. Such research will contribute to the ongoing research related to FRGCs by extending the available database results.

2. Theoretical Criteria for Deflection Hardening Behavior

As shown in Fig. 1, the typical deflection hardening behavior is mainly characterized by two points called limit of proportion (LOP) and modulus of rupture (MOR). According to ASTM C1018 [35], the LOP point is defined as the point where the load-deflection curve nonlinearity becomes conspicuous; in other words, such point represents the first cracking load. However, the identification of such a point can be challenging in the fibrous composites exhibiting deflection hardening behavior; thus, the method proposed by Kim et al. [36] was followed in this study. The MOR point, or else known as the ultimate flexural strength, is defined as the point following the LOP where the softening starts to occur afterward. P_{LOP} and P_{MOR} are representing the cracking and ultimate loads, respectively; while their corresponding deflections are labeled as δ_{LOP} and δ_{MOR} , respectively, as shown in Fig. 1.

Two conditions shall be satisfied in order to assure the deflection hardening behavior of a composite. First, the ultimate load (P_{MOR}) must be larger than the cracking load (P_{LOP}). Second, the deflection at ultimate (δ_{MOR}) needs to exceed that at first cracking (δ_{LOP}). The higher the gap between the cracking and ultimate loads and deflections, the better deflection hardening behavior and ductility can be achieved. Accordingly, this concept can be interpreted into a new value called the “ductility index (DI)” which is the ratio of δ_{MOR} to δ_{LOP} . The ductility of a composite is directly related to its DI value; in other words, the higher the DI value is, the more ductile the composite will be.

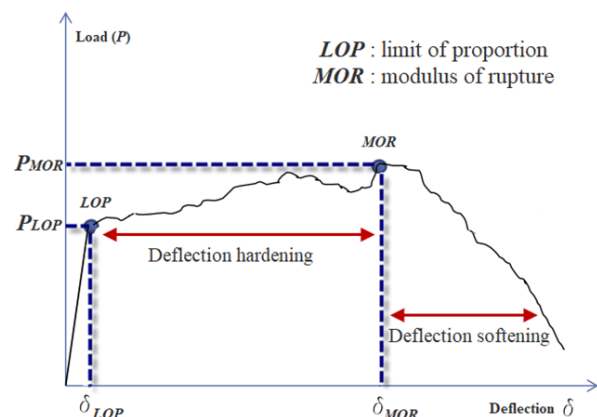


Fig. 1. Typical deflection hardening behavior of composites

3. Materials

For geopolymer matrix preparation, local Hong Kong low-calcium Class-F fly ash (FA) and

ground granulated blast-furnace slag (GGBS) imported from mainland China were used in this study. The chemical compositions of the precursor materials are reported in Table 1, as determined by X-ray Fluorescence (XRF) test. Fig. 2 shows the morphologies of the raw precursor materials using scanning electron microscope (SEM) wherein the FA particles were spherical in shape with a relatively high content of irregular shaped glassy contents, while the GGBS particles were mainly anomalous. Figs. 3 a

and b display the X-ray Diffraction (XRD) patterns and the particle size distribution of the raw precursor materials, respectively. Clearly, the FA contained relatively high crystalline content while relatively large amorphous hump was noticed in the GGBS XRD pattern. The GGBS particle size was relatively larger than that of FA particles where the d_{50} values of GGBS and FA were 13 and 24 microns, respectively.

Table 1– Chemical composition of fly ash and slag determined by XRF

Parameters (% by weight)	SiO ₂	Al ₂ O ₃	CaO	Fe ₂ O ₃	MgO	SO ₃	TiO ₂	K ₂ O	P ₂ O ₅	SrO	LOI ^a
FA	44.4	32.6	6.67	6.49	1.86	2.27	1.24	1.81	0.44	0.14	5.55
GGBS	18.9	6.43	66.9	0.74	1.41	1.97	1.88	0.67	0.08	0.18	0.25

^a Loss on ignition

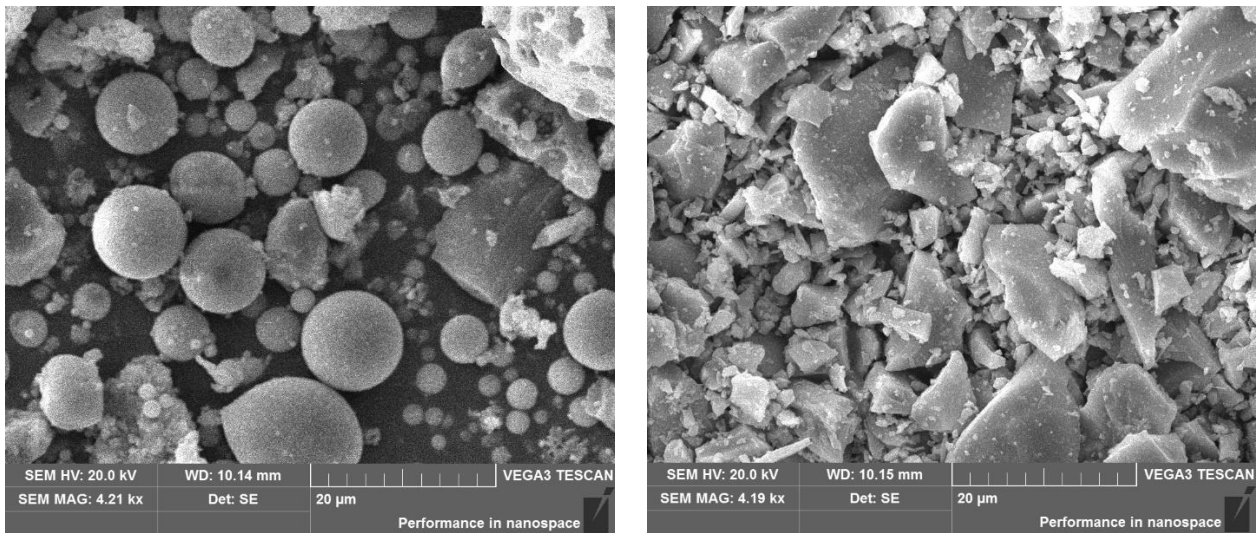


Fig. 2 – The morphology of raw precursor materials: a) FA and b) GGBS

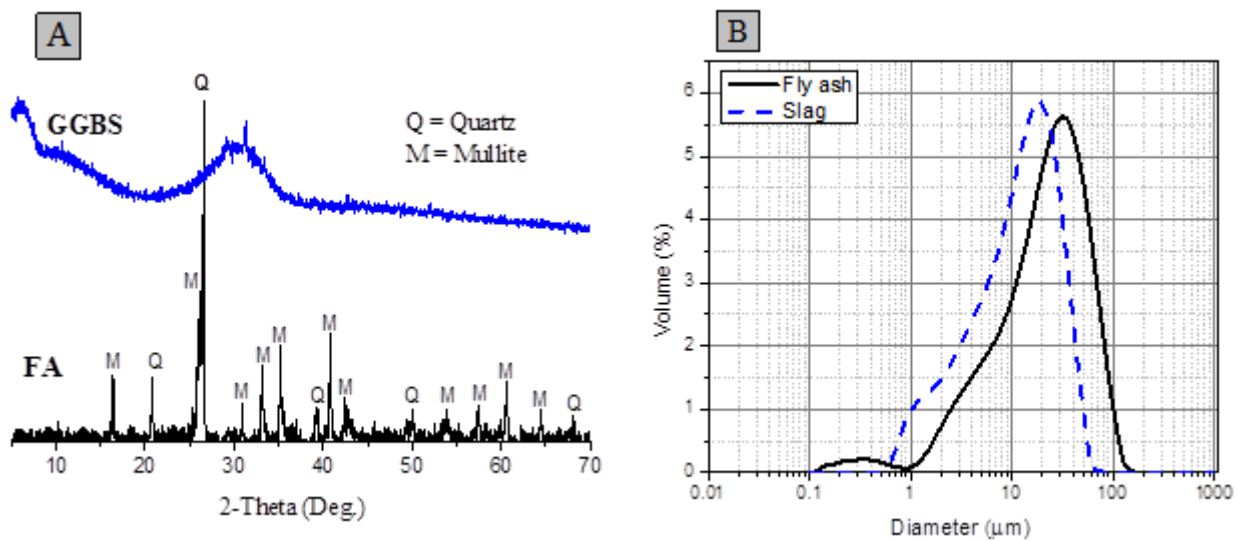


Fig. 3 – Raw precursor materials properties: a) XRD patterns and b) particle size distribution

Table 2– Properties of fibers

Fiber type	Length (mm)	Diameter (μm)	Modulus of elasticity (GPa)	Strength (MPa)	Density (g/cm^3)
ST	13	180	200	2850	7.8
PE	13	17	114	3000	0.97

Table 3– Mix proportions (by wt.) and fiber content

Series	Mix ID	Hybridization %		Binder		Activator /Binder	Water /Binder	Sand /Binder
		PE	ST	Slag	Fly ash			
1	P: FRGC-S	2.0%	0.0%	1	-	0.12 ^a	0.45	-
		1.5%	0.5%					
		1.0%	1.0%					
		0.5%	1.5%					
		0.0%	2.0%					
2	P: FRGC-FA/S	2.0%	0.0%	0.5	0.5	0.12 ^a	0.45	-
		1.5%	0.5%					
		1.0%	1.0%					
		0.5%	1.5%					
		0.0%	2.0%					
3	M: FRGC-S	1.5%	0.5%	1	-	0.12 ^a	0.45	0.3 ^b
	M: FRGC-FA/S	1.5%	0.5%	0.5	0.5	0.12 ^a	0.45	0.3 ^b

^a anhydrous sodium metasilicate powder

^b with a maximum size of 212 μm

In order to produce the one-part geopolymer matrix, the solid alkali activator used was anhydrous sodium metasilicate powder based on the recommendation of Nematollahi, et al. [31]. The anhydrous sodium metasilicate powder composed of 50.46% Na_2O and 47.24% SiO_2 by weight; accordingly, the modulus ratio (M_s) of such activator was 0.94 (where $M_s = \text{SiO}_2/\text{Na}_2\text{O}$).

The fibers used in this study were copper-coated straight-shaped steel fibers (ST) and ultra-high molecular weight polyethylene fibers (PE). Table 2 presents the mechanical properties of both fibers as provided by the manufacturers.

Fine silica sand with a maximum size of 212 μm imported from mainland China was used in this study which was adapted from Nematollahi, et al. [26]. It is good to mention that such small sand size was chosen to minimize the fracture toughness and first cracking strength of the geopolymer matrix which is beneficial for the deflection hardening behavior of the composite [16].

4. Experimental Program

The deflection hardening behavior and the elastic modulus of one-part steel-polyethylene FRGCs were experimentally investigated in this study. The effects of different hybridization ratios, different precursor materials (e.g. 100% GGBS matrix and 50/50

FA/GGBS matrix) and sand addition were also highlighted.

4.1 Mix proportions, procedure, casting and curing

The experimental mix proportions and fiber contents followed in this paper were similar to those mentioned in Alrefaei and Dai [16] as shown in Table 3. The precursors used to produce the FRGCs were 100% GGBS and a blend of 50% fly ash with 50% GGBS in Series 1 and 2, respectively. Five different hybrid combinations ranging between 0% to 2% of ST and PE fibers were used in both Series 1 and 2 while the total fiber volume fraction was kept at 2%. Series 3 included the hybrid composite of 1.5% PE and 0.5% ST with both slag-based and blended-based geopolymer matrix in addition to the 212 μm fine sand. As shown in Table 3, the sand and the activator contents used in this study were 30% and 12%, respectively, resulting in an alkali concentration (Na_2O % by the mass of binder) of 6%. The sand content was adapted from Nematollahi, et al. [26] while the activator content was recommended by Alrefaei and Dai [16]. Tap water was used in all the mixes and the sand was oven-dried before usage. The water-to-binder ratio used in all FRGC mixes was 0.45 which was equivalent to a liquid-to-solid ratio of 0.4 with the aim of guaranteeing good workability and better fiber dispersion in the composites.

The codified mix ID includes three alphanumeric character parts at which the first part mentions the geopolymer matrix: “P” for paste and “M” for mortar, the second part symbolizes the fiber-reinforced geopolymer composite shortcut “FRGC” and

finally the third part specifies the precursor used to synthesize the geopolymer matrix: “S” for slag and “FA/S” for blended geopolymer composites.

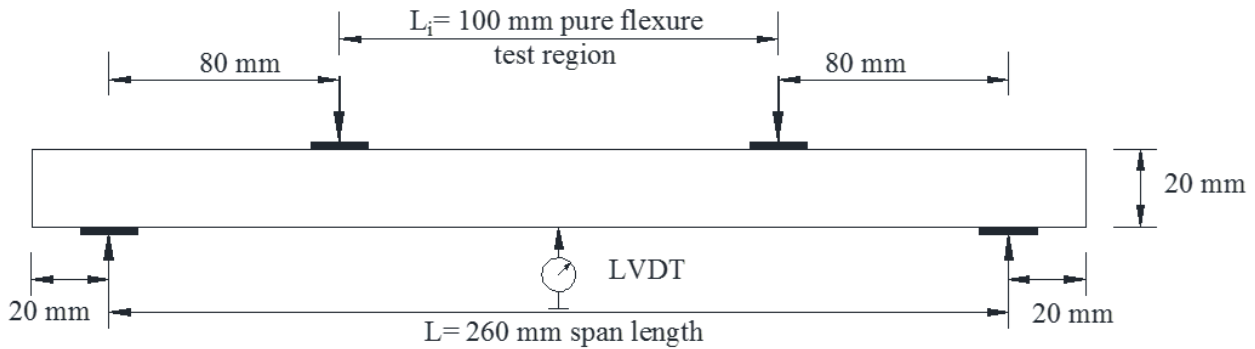


Fig. 4 – Schematic of bending test set-up

Four sheet specimens in addition to four cylinders were cast for each FRGC mix. The sheet specimens were 300 mm, 75 mm and 20 mm in length, width, and thickness, respectively. The cylinders were 50 mm and 150 mm in diameter and height, respectively. Hobart mixer was used to prepare all the FRGC within 15 to 20 minutes duration. The mixing procedure of geopolymer matrix and fiber addition techniques were adapted from Alrefaei & Dai [16] and Alrefaei, et al. [37], respectively. All the specimens were prepared and cast using a single batch. A mechanical vibrating table was used to compact the FRGC samples following Alrefaei, et al. recommendations [37] wherein mono-steel composites were not over vibrated to prevent fiber segregation. To avoid drying shrinkage cracks, all the specimens were covered with wet burlap and plastic sheets for 24 hours after casting. The specimens were demolded after 24 hours then placed in a water tank for the next 27 days. All the tests were conducted at the age of 28 days.

4.2 Instrumentation and testing procedures

Four points bending test was used to study the deflection hardening behavior of the achieved FRGCs. The schematic of the bending test set-up and sheet specimen dimensions are shown in Fig. 4. A universal testing machine was used to test the sheet specimens with an extension control rate of 0.5 mm per minute [22]. A 50 mm capacity LVDT was used to measure the mid-span deflection during the bending test. The flexural strength was calculated using the following equation [38]:

$$\sigma = \frac{3P(L-L_i)}{2bd^2} \dots\dots\dots (1)$$

where σ is flexural stress; P is the load; L is the length of the support span (260 mm); L_i is the length of the loading span (100 mm); b is the width (75 mm)

and d is thickness (20 mm) of the sample. The ductility index (DI) was calculated using the following equation [22]:

$$DI = \frac{\delta_{MOR}}{\delta_{LOP}} \dots\dots\dots (2)$$

where δ_{MOR} is the deflection at ultimate peak load and δ_{LOP} is the deflection at first cracking load.

The cylinders were tested in compression using a hydraulic testing machine with an extension control rate of 0.03 mm per minute in accordance with ASTM C39 [39], while the elastic modulus was calculated using the equation mentioned in ASTM C469 [40]. The change of the cylinder’s length was measured over a gauge length of 100 mm. All the samples were capped using gypsum in compliance with ASTM C617 [41]. The cylinder test setup is shown in Fig. 5.

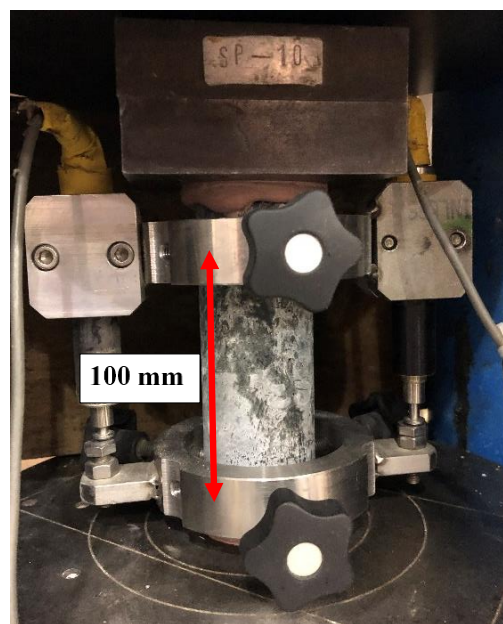


Fig. 5 – Test set-up of cylinder compression

5. Results, Analysis, and Discussion

All experimental test results (i.e. Average \pm Standard Deviation) are briefed in Table 4. The discussion and analysis of the results will be carried out

in detail in the following sections. The error bars were not included in some figures in this paper to maintain clarity.

Table 4 – Summary of test results

Series	Mix ID	Fiber content (%)		Composites properties											
		PE	ST	s_{LOP} (MPa)	δ_{LOP} (mm)	s_{MOR} (MPa)	δ_{MOR} (mm)	DI	No. of cracks	S (mm)	f_{cu} (MPa)	f_c' (MPa)	E (GPa)	$f_c'm$ (MPa)	E_m (GPa)
1	P: FRG C-S	2.0 %	0.0 %	2.7 \pm 0.4	1.0 \pm 0.2	8.2 \pm 1.7	27.1 \pm 4.3	27.5 \pm 9.3	69	2.9	59 \pm 5.6	44.3 \pm 4.2	26.1 \pm 1.6	----	----
		1.5 %	0.5 %	2.8 \pm 0.3	0.7 \pm 0.1	4.2 \pm 0.3	12.5 \pm 7.6	18.6 \pm 10	38	4.2	63.3 \pm 1.2	48.1 \pm 5.6	26.5 \pm 1.9		
		1.0 %	1.0 %	4.5 \pm 0.8	1.2 \pm 0.3	6.9 \pm 1.4	13 \pm 7.0	9.94 \pm 4.8	29	7	63 \pm 4.4	67.6 \pm 1.9	28.3 \pm 2.4		
		0.5 %	1.5 %	6.8 \pm 0.9	1.3 \pm 0.1	8.5 \pm 1.5	4.3 \pm 0.9	3.3 \pm 0.7	7	21	73.1 \pm 5.6	74.4 \pm 1.3	25.8 \pm 1.3		
		0.0 %	2.0 %	6.2 \pm 0.3	1.2 \pm 0.3	8.3 \pm 0.7	2.4 \pm 0.5	2.0 \pm 0.2	1	---	61.5 \pm 4.6	60.3 \pm 3.2	29.9 \pm 2.2		
2	P: FRG C- FA/S	2.0 %	0.0 %	3.0 \pm 1.0	1.2 \pm 0.1	7.5 \pm 0.4	22.2 \pm 1.8	18.6 \pm 1.4	54	3.3	60.6 \pm 2.2	61.6 \pm 2.2	24.7 \pm 1.1	56.3 \pm 1.8	25 \pm 1.1
		1.5 %	0.5 %	3.2 \pm 0.8	0.8 \pm 0.1	6.9 \pm 1.4	11.1 \pm 5.4	13 \pm 5	25	5.9	60.6 \pm 3.5	66.6 \pm 4.5	26.6 \pm 0.6		
		1.0 %	1.0 %	3.6 \pm 0.6	0.97 \pm 0.1	6.9 \pm 2.1	9.8 \pm 4.9	10.2 \pm 4.8	15	4.3	70.8 \pm 3.1	71.6 \pm 2.6	27.1 \pm 0.4		
		0.5 %	1.5 %	3.4 \pm 0.4	1.0 \pm 0.2	7.3 \pm 1.5	8.9 \pm 1.4	9.1 \pm 1.8	7	30	83.9 \pm 6.2	82.3 \pm 4.3	23.2 \pm 0.6		
		0.0 %	2.0 %	4.3 \pm 0.5	0.8 \pm 0.1	6.6 \pm 1.3	1.8 \pm 0.5	2.1 \pm 0.4	1	---	76.6 \pm 3.4	80.5 \pm 3.1	26.6 \pm 0.3		
3	M: FRG C-S	1.5 %	0.5 %	4.5 \pm 0.7	1.0 \pm 0.2	6.9 \pm 0.9	12.7 \pm 4.4	12.6 \pm 4.9	41	4.1	62.5 \pm 2.6	64.8 \pm 3.1	31 \pm 1.4	----	----
	M: FRG C- FA/S	1.5 %	0.5 %	4.3 \pm 1.5	1.1 \pm 0.6	7.3 \pm 0.9	17.7 \pm 5.2	19.3 \pm 8.7	47	4.1	64.7 \pm 1.2	69.4 \pm 3.1	31.6 \pm 0.8	67.4 \pm 0.4	27 \pm 0.5

Note: The numbers indicate Average \pm Standard Deviation

5.1 Compressive strength and elastic modulus

Generally, as reported in Table 4, the cylinders' compressive strengths (f_c') were 1% to 10% higher compared to the cubes' compressive strengths (f_{cu}). However, some composites showed a contrasting trend where the compressive strength of the cubes was up to 25% greater relative to that of the cylinders; thus, now general conclusion could be drawn. It is good to highlight that the compressive strength and elastic modulus results of the none-fibrous slag-based cylinders (i.e. paste and mortar) were not provided in Table 4. It was challenging to test such matrices since the cast samples were highly brittle, and most of the samples were already broken before testing due to the rapid volume change caused by the high content of slag. On the other hand, the blended-based geopolymer matrix achieved cylinders' compressive strength and elastic modulus of 56 MPa and 25 GPa, respectively. The sand addition occasioned 20% and 8% increases in both cylinders' compres-

sive strength (i.e. from 56 MPa to 67 MPa) and elastic modulus (i.e. from 25 GPa to 27 GPa) of the blended geopolymer matrix, respectively. Such observation was in consistency with previous research [16].

Fig. 6 shows the relationship between the cylinders' compressive strength and the hybrid combinations for all the FRGCs achieved in this study. As shown in Fig. 6 and reported in Table 4, the cylinders' compressive strength of the FA/S composites ranged from 61 to 82 MPa depending on the hybrid combination incorporated in the matrix, while the slag composites attained cylinders' compressive strength ranging from 44 to 74 MPa. Thus, it was found that the incorporation of FA in the slag-based geopolymer matrix improved the compressive strength of the P:FRGC-FA/S by 6% to 38% relative to the P:FRGC-S composites. This could be due to the high volume change and drying shrinkage rate of the slag-based geopolymer matrix relative to that of FA/S geopolymer which might degrade the compressive

strength of the FRGC [42, 43]. Further, it was observed that the compressive strength of the FRGCs was directly related to the ST fiber volume fraction included in the composite which is supported by previous research results [16, 37]. The inclusion of fibers in the FA/S geopolymer matrix seemed to improve the cylinders' compressive strength since all the P:FRGC-FA/S composites showed a higher compressive strength relative to their corresponding matrix (i.e. P:FRGC-FA/S matrix). On the other hand, it is worth mentioning that the mono-ST composites achieved a relatively lower compressive strength relative to the 0.5%PE+1.5%ST composites which might be due to the ST fiber settlement during the compaction process of the mono-ST composites. A similar observation was reported in previous research related to ECC [37]. Such a phenomenon was more severe in the slag-based geopolymer compared to FA/S geopolymer since the slag-based geopolymer showed weaker thixotropic behavior (i.e. less viscous) relative to that of FA/S geopolymer which might cause uncontrollable adverse fiber segregation.

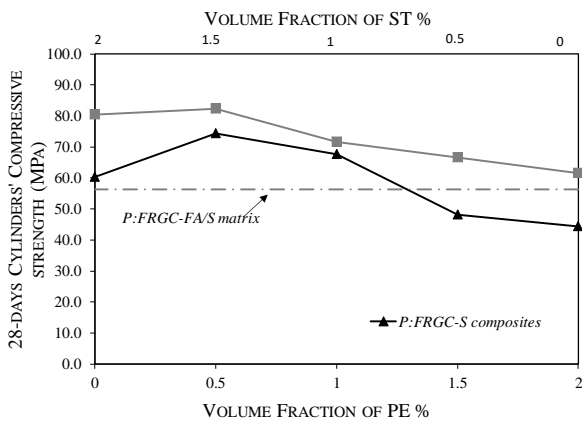


Fig. 6 – 28-days cylinders' compressive strength versus PE and ST fiber volume fractions

Fig. 7 plots the elastic modulus results for the achieved FRGCs in this study. Clearly, the elastic modulus exhibited an opposite trend to that observed in the compressive strength (i.e. refer to Fig. 6). In other words, the elastic modulus of FA/S FRGCs was lower than that of slag-based FRGCs although the FA/S FRGCs achieved relatively larger compressive strength compared to the slag-based FRGCs. According to previous research [44], the elastic modulus of C-A-S-H gels in the slag-based geopolymer is higher than that of N-A-S-H gels in the FA-based geopolymer. The elastic modulus of P:FRGC-S composites was in the range of 26-30 GPa, while P:FRGC-FA/S composites had an elastic modulus ranging from 23-27 GPa depending on the fiber combination included in the matrix. The general trend observed in Fig. 7 was the more ST fibers included in the matrix, the higher the composite elastic modulus will be, to a limited extent. Further, the fiber addition improved the elastic modulus of the corresponding matrix regardless of the fiber type (i.e. P:FRGC-FA/S composites showed higher E compared to P:FRGC-FA/S matrix, except the 0.5%PE+1.5%ST). It's good to mention that the experimental values of elastic modulus observed in this study were significantly larger than their corresponding theoretical values (i.e. calculated based on the effective crack model theory [45]) reported in previous research [16, 21, 25]. Further, all the FRGC cylinders maintained their shape after the compression test (refer to Fig. 8) due to the PE fiber bridging effect [12, 16].

ulus will be, to a limited extent. Further, the fiber addition improved the elastic modulus of the corresponding matrix regardless of the fiber type (i.e. P:FRGC-FA/S composites showed higher E compared to P:FRGC-FA/S matrix, except the 0.5%PE+1.5%ST). It's good to mention that the experimental values of elastic modulus observed in this study were significantly larger than their corresponding theoretical values (i.e. calculated based on the effective crack model theory [45]) reported in previous research [16, 21, 25]. Further, all the FRGC cylinders maintained their shape after the compression test (refer to Fig. 8) due to the PE fiber bridging effect [12, 16].

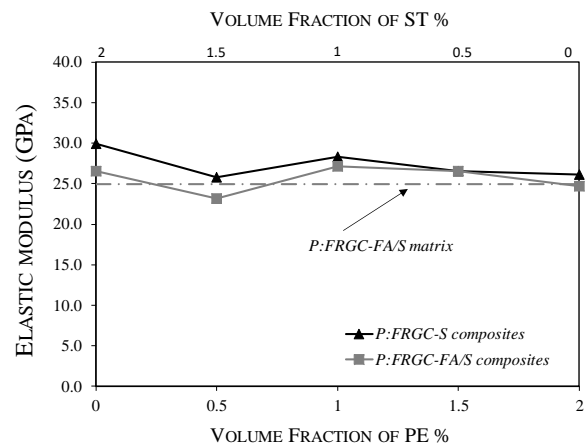


Fig. 7 – Elastic modulus of FRGC

Fig. 9 indicates the effect of sand addition on the compressive strength and elastic modulus of 1.5%PE+0.5%ST composite when included in both blended-based and slag-based FRGC. Clearly, the sand addition improved both compressive strength and elastic modulus of both FA/S and slag-based 1.5%PE+0.5%ST FRGCs. The improvements of the matrices compressive strength after sand addition were 4% and 35% for FA/S and slag-based FRGCs, respectively.

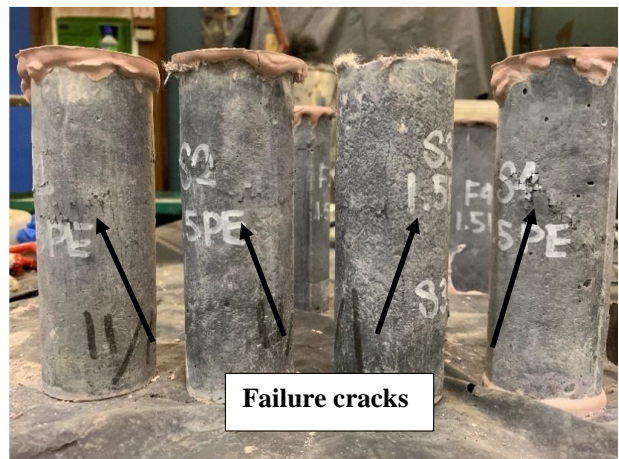


Fig. 8 – FRGC cylinders after compression test

Besides, the elastic modulus was enhanced by 19% when the sand was incorporated in both FA/S and slag-based 1.5%PE+0.5%ST FRGCs. According to previous studies [16, 26], sand addition improved the fracture properties of the geopolymer matrix significantly and thus increased their theoretical E .

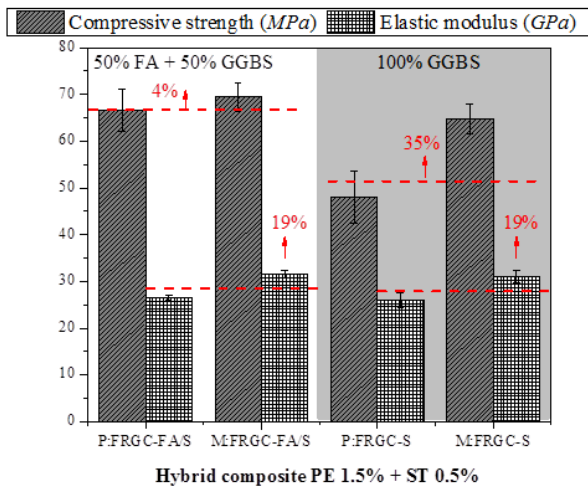


Fig. 9 – Effect of sand addition on compressive strength and elastic modulus of 1.5% PE and 0.5% ST composite

5.2 Flexural response

5.2.1 Cracking and ultimate strengths

Figs. 10 a and b plot the flexural responses of both slag and blended FRGCs respectively. It is good to mention that the responses in Fig. 10 are the average of 4 specimens for each group at which the average curve presents the lowest deflection value in each group. Generally, the flexural responses of hybrid FRGCs laid between the envelope of mono FRGCs at which similar observations were reported for the tensile response in a previous study of the authors [16]. It is good to mention that the mono-PE FRGC attained a relatively nearby ultimate flexural strength to that of mono-ST FRGC when the binder was 100% slag (refer to Fig. 10a), while the ultimate flexural strength of the mono-PE blended-based FRGC outperformed that of mono-ST FRGC of the same matrix. Such observations might raise some doubts regarding the effectiveness of the hybridization concept in geopolymer composites relative to the cementitious one (FRGCs) wherein the effect of such a concept was more noticeable [46]. This could be due to the better interfacial strength between ST fiber and the cementitious matrix relative to that of geopolymer one [18]. However, it was challenging to capture the general trend following the average responses shown in Fig. 10, thus the flexural cracking and ultimate strengths reported in Table 4 are plotted in Fig. 11 for better comparison. In general, it was

found that the slag-based FRGCs attained a relatively higher flexural cracking strengths in reference with the blended-based FRGCs (i.e. for 2% and 1.5% PE blended composites showed slightly higher cracking strength relative to slag composites). Such observation was identical to that of the tensile cracking strengths reported in previous research [16] at which the slag-based FRGCs showed higher cracking strengths relative to blended-based FRGC except for the composites including a higher fraction of PE fibers (i.e. PE volume $\geq 1.5\%$). Further, the flexural cracking strength of the slag-based FRGCs was directly related to the ST volume included in the composite which is in consistence with previous research [16]. On the other hand, the hybrid combinations did not show any effect on the flexural cracking strength of the blended-based FRGCs unlike the direct tensile cracking strength of the same composites reported in [16]. The reason for such behavior could be related to the fracture toughness of the slag- and blended-based geopolymer matrices reported in the previous study of the authors [16]. The higher toughness of the blended-based geopolymer matrix relative to the slag-based one (i.e. K_m and J_{tip} as reported in [16]) could justify why the former had a higher cracking strength compared for the latter for composites with PE volume $\geq 1.5\%$. However, the use of higher content of ST (i.e ST volume $\geq 1\%$) has compensated the lower fracture toughness of the slag-based geopolymer matrix and therefore the slag-based FRGC attained a higher flexural cracking strength compared to blended-based FRGC when ST volume was $\geq 1\%$.

Additionally, the ultimate flexural strengths showed a similar trend to that of the flexural cracking strengths. In general, the slag-based FRGCs outperformed the blended-based FRGCs in terms of the ultimate flexural strength (i.e. except the 1.5%PE+0.5%ST composite was off this trend). The reason for such behavior could be due to the more compacted geopolymer matrix of slag-based FRGC compared to that of blended-based FRGC. As a result, the fiber-matrix bond of the slag-based FRGC would be higher than that of the blended-based FRGC, which contributed to the higher flexural and tensile strength of slag-based FRGC [16]. Further, the ultimate flexural strength of the slag-based FRGCs was dependent on the ST volume included in the matrix to a limited extent; however, the mono-PE composite showed a comparable ultimate flexural strength to that of the high-volume ST composite (i.e. ST ≥ 1.5) in case of slag-based geopolymer matrix. Therefore, the hybrid combinations showed a poor performance in the slag-based geopolymers in terms of the ultimate flexural strength. On the other hand, such hybrid combinations showed a negligible effect on the flexural ultimate strength of the blended-

based FRGCs. It is worth highlighting that the observed behavior of the flexural response was unlike that of the direct tensile response reported in Alrefaei and Dai [16]. In other words, the flexural response of

slag-based FRGCs was relatively alike the direct tensile response of blended-based FRGCs and vice versa (refer to Fig. 11 in [16]).

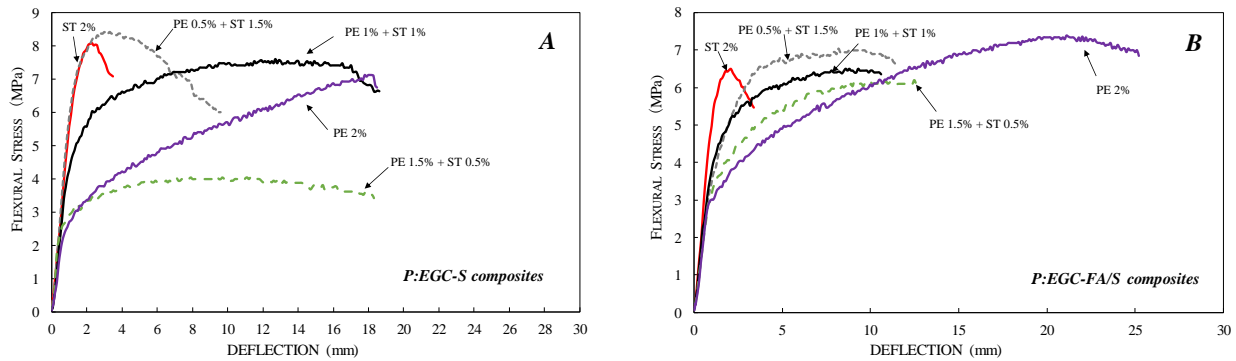


Fig. 10 – Deflection hardening behavior of the hybrid composites: a) slag FRGC b) blended FRGC

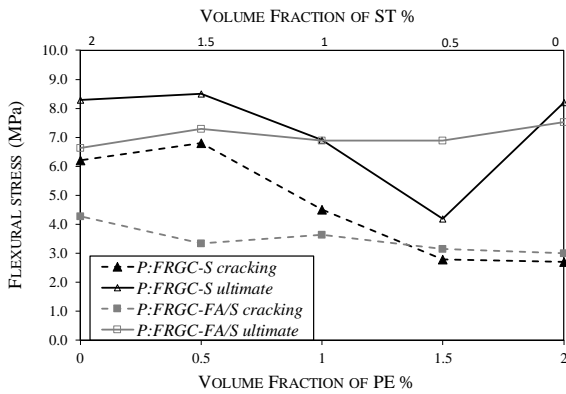


Fig. 11 – Cracking and ultimate flexural stresses versus PE and ST fiber volume fractions

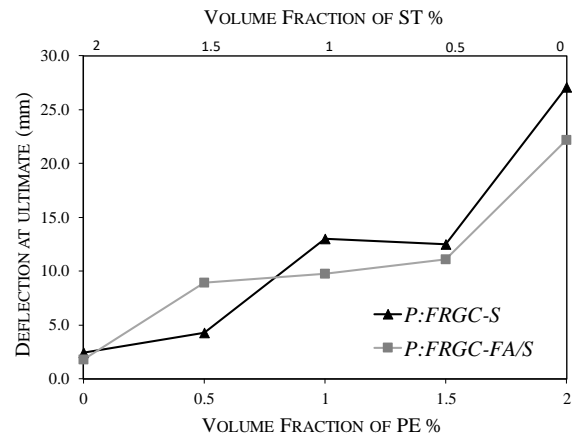


Fig. 12 – Deflection at ultimate load versus PE and ST fiber volume fractions

5.2.2 Deflections and ductility indices

Fig. 12 illustrates the relationship between the deflection at ultimate load versus ST and PE fiber volume fractions for both slag and blended FRGCs. It was found that the PE volume fraction greatly influenced the deflection capacity of FRGC composites at ultimate flexural strength which is in agreement with previous studies [46, 47]. In addition, it was observed that the slag-based FRGCs exhibited relatively larger deflections at ultimate relative to the blended-based FRGCs (i.e. except 1.5%PE+0.5%ST composite). For example, the mono-PE slag-based composite achieved a deflection of 27 mm at the ultimate load, which is 22% higher than that of the mono-PE blended-based composite (i.e. 22 mm). Such observations were consistent with previous research findings [16] (i.e. refer to Fig. 13 in [16]). This could be due to the lower cracking strength of the slag-based FRGCs relative to blended-based FRGCs when the mono-PE combination was included in the matrix, which is more favorable for the pseudo strain hardening behavior [16].

However, for better understanding the effect of hybridization on the ductility of the FRGCs, Fig. 13 plots the calculated ductility indices (using equation 2 in section 3.2) versus the ST and PE volume fractions. Clearly, the ductility index of the composites was also directly related to the PE volume included in the FRGCs. In other words, the higher the PE volume in the composite, the more ductile (i.e. higher ductility index) the composite will be. However, it was challenging to decide which geopolymer matrix had a better ductility when incorporated with the hybrid combinations since the two curves in Fig. 13 almost intersect at the point of 1% PE. In general, the blended-based geopolymer matrix showed a higher DI for $PE \leq 1$, while the slag-based geopolymer matrix was more ductile for $PE > 1$. Therefore, no clear conclusion could be drawn.

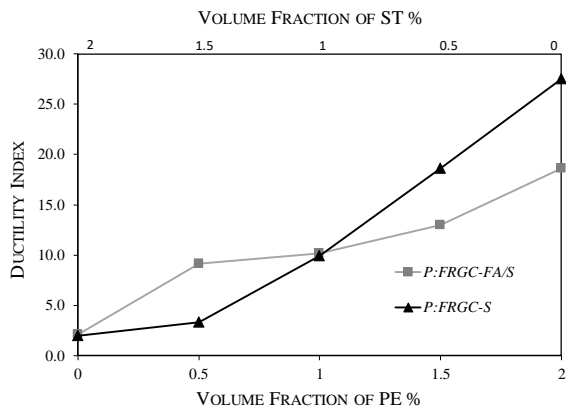


Fig. 13 – Deflection at ultimate load versus PE and ST fiber volume fractions

5.3 Effect of sand addition

Fig. 14 displays the effect of 212 μm sand addition on the deflection hardening behavior of the hybrid composite PE 1.5% and ST 0.5% when incorporated in both slag-based and blended-based geopolymer matrices. As shown in Fig.14, the addition of sand was found to increase both cracking and ultimate flexural strengths of both slag-based and blended-based FRGCs. A similar observation was reported in both cementitious composites (ECCs) [47] and geopolymer composites [16, 26]. However, in order to summarize the effect of sand addition on the behavior of FRGCs, the average values reported in Table 4 are plotted in Fig. 15. As previously mentioned, the sand addition improved the flexural cracking strength of both blended- and slag-based FRGCs by 34% and 60%, respectively, while the ultimate flexural strength was enhanced by 6% and 64% for both blended- and slag-based FRGCs, respectively, in reference with their corresponding paste composites. On the other hand, the sand addition unexpectedly improved the ductility and deflection capacity of both blended- and slag-based FRGCs. However, the deflection improvement after sand addition was more noticeable in the blended-based FRGC (i.e. 59% increase in the deflection relative to the corresponding paste) compared to the slag-based FRGC (i.e. almost no change observed in the deflection capacity relative to the corresponding paste). Such improvement in the deflection behavior could be explained according to Nematollahi, et al. [26] research at which the use of appropriate content of fine sand (i.e. 212 μm) was found to maintain a desirable strain hardening behavior of FRGCs. Furthermore, the addition of sand has reduced the high volume change and drying shrinkage rate of the geopolymer paste matrices which might be the reason why the sand addition has improved the deflection behavior of geopolymer composites. Similar behavior can be observed in UHP-ECC at which the fine sand is used to minimize the shrinkage of the cementitious matrix [3]. However, such observation contradicted with the

general trend of previous research wherein the sand addition adversely affects the strain (i.e. deflection) hardening behavior of composites due to the detrimental increase in the matrix fracture toughness that violates the pseudo strain hardening conditions [37, 48].

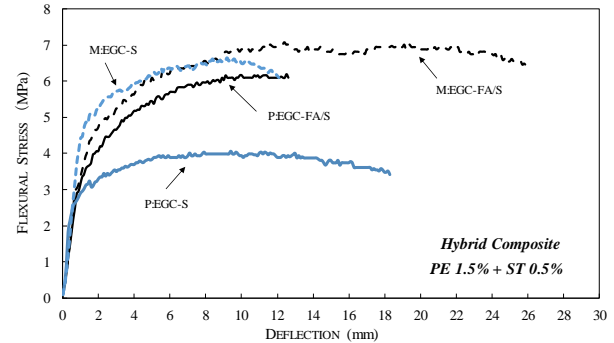


Fig. 14 – Effect of 212 μm sand addition on the deflection hardening behavior of the hybrid composite PE 1.5% and ST 0.5% with different FRGC matrices

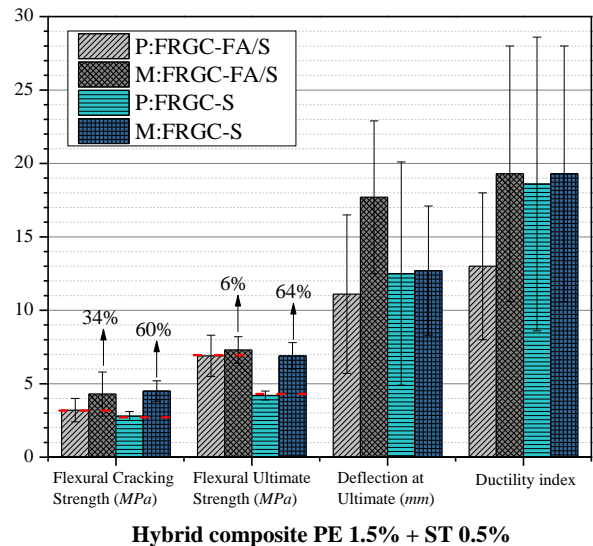


Fig. 15 – Summary of 212 μm sand addition effect on the flexural response of the hybrid composite PE 1.5% and ST 0.5% with different FRGC matrices

5.4 Cracking behavior

Fig. 16 shows the schematic representations of all FRGCs’ final conditions (i.e. over the full length of the specimen 300 mm) after testing wherein the numbers of the cracks passing the imaginary center line in each specimen are reported in the square brackets. It is good to mention that the reported cracked samples shown in Fig. 16 are based on the most cracked specimen from each group. All the cracks were marked using permanent marker after reaching the ultimate load and unloading the specimens; therefore, the actual number of cracks might be higher than the reported one since many micro-cracks were closed after unloading the specimens which made it difficult to trace all the cracks [49, 50].

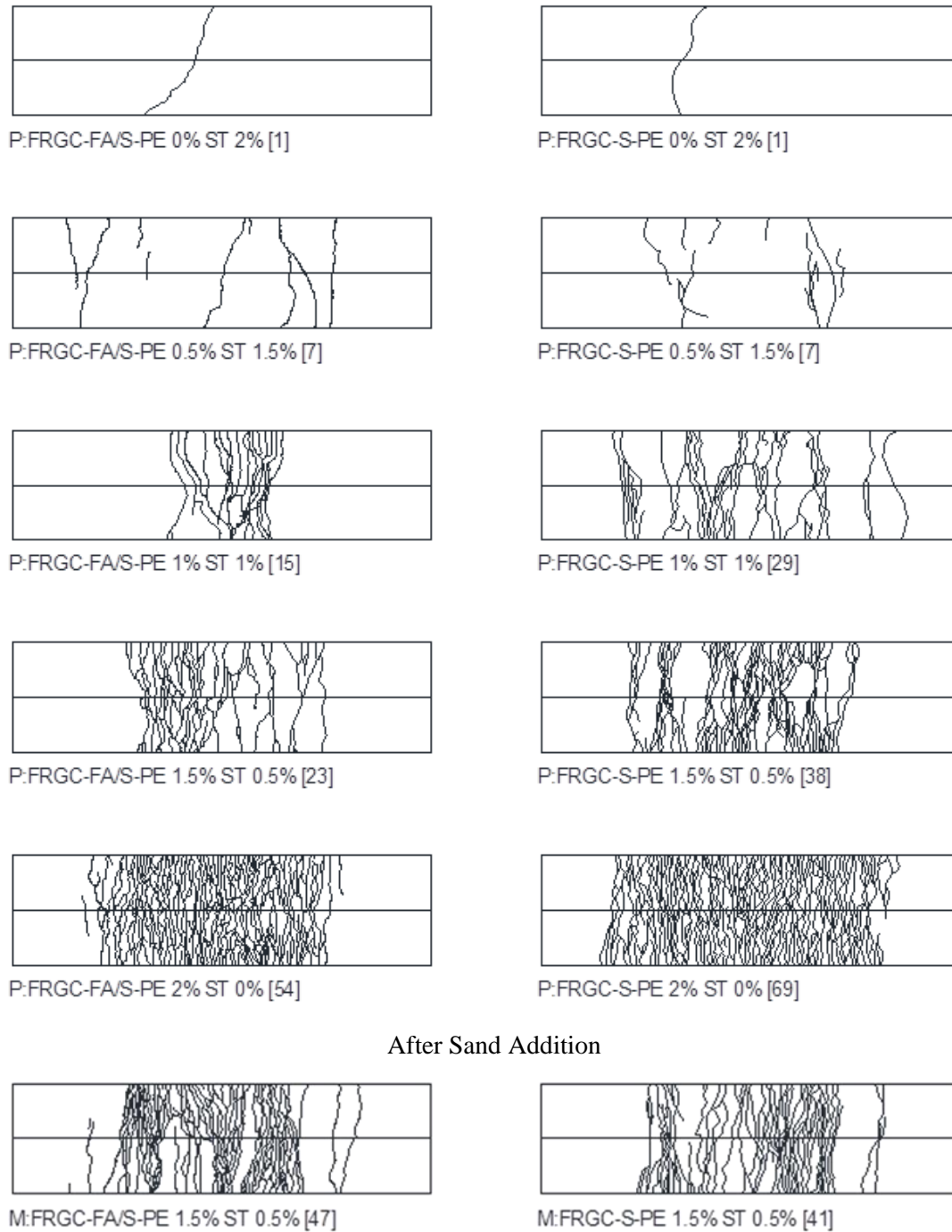


Fig. 16 – Deflection cracking behavior of hybrid fiber FRGCs (The number shown in square brackets [] represents the number of the cracks).

Generally, the multiple-cracking behavior of the FRGCs was significantly reliable on the PE volume fraction incorporated in the composites. In other words, the higher the PE volume included in the matrix, the more saturated the multiple-cracking behavior will be. Such observation was previously recorded in both ECCs [37, 46, 47] and EGCs [16, 25]. As shown in Fig. 16, it was observed that the absence

of PE fibers resulted in a highly brittle flexural failure with a single major crack (i.e. mono-ST FRGCs). Further, the number of cracks achieved by the slag-based FRGCs was relatively higher than that presented by the blended-based FRGCs. On the other hand, the multiple-cracking behavior of the 1.5%PE+0.5%ST composite was relatively enhanced after the addition of the sand to both slag- and

blended-based FRGCs. This was in consistence with the observation reported by Nematollahi, et al. [26] wherein the use relatively low-volume small-size sand (i.e. 30% of 212 μm sand by weight of binder) was found to improve the cracking behavior in addition to elastic modulus, ultimate strength, and strain capacity. However, the bulk of previous research mentioned that the sand addition violates the pseudo strain hardening conditions which in turn adversely affects the cracking behavior of the composite [16, 37, 47, 48].

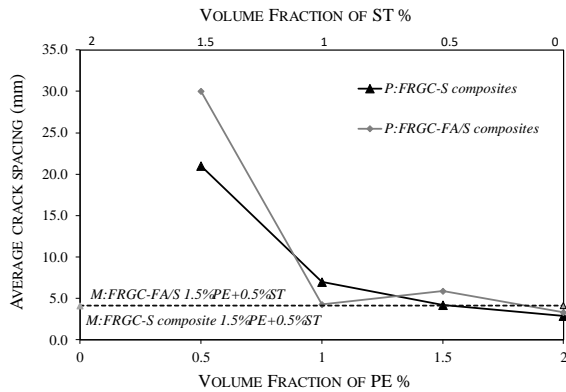


Fig. 17 – Average flexural crack spacing for all FRGCs

In order to better understand the flexural cracking behavior of FRGCs, the crack spacing (S) was calculated by dividing the distance between the farthest cracks over the number of cracks minus 1 ($n-1$) as mention in Alrefaei & Dai [16]. The calculated crack spacings are reported in Table 4 and presented in Fig. 17. As shown in Fig.17, the crack spacing dropped significantly by the addition of PE fibers to the geopolymer matrix. When the PE volume fraction was higher than 1%, the decrease of crack spacing was modest to a limited extent. This might confirm that the critical PE volume fraction was about 1% as reported by a previous study [18]. In addition, the crack spacing was found to be lower in slag-based FRGCs relative to that of blended-based FRGCs which is expected as the number of cracks was comparatively higher in slag-based FRGCs in reference with the blended-based FRGCs. After sand addition, the crack spacing was identical in both slag- and blended-based FRGCs (i.e. 4.1 mm as reported in Table 4) which was lower than that of their corresponding paste composites (i.e. 4.2 and 5.9 mm for P:FRGC-S and P: FRGC-FA/S respectively). This confirmed that the mortar composites (i.e. with sand) maintained a comparable crack spacing with the paste composites (i.e. without sand).

6. Summary and Conclusions

This study reports the experimental results of elastic modulus in addition to the deflection hardening behavior of the ambient-cured one-part steel-polyethylene FRGCs. Based on the observed results, the following conclusions can be summarized:

- 1) The inclusion of fibers improved the elastic modulus of the FRGCs relative to their corresponding none-fibrous matrices. Such improvements in the elastic modulus of FRGCs were directly related to the ST volume fraction included in the composite.
- 2) The slag-based FRGCs showed a relatively higher elastic modulus although they exhibited lower cylinders' compressive strength relative to the blended-based FRGCs.
- 3) Generally, the flexural behavior of the slag-based FRGCs (i.e. modulus of rupture, deflection capacity, and multiple-cracking behavior) was comparatively better than that of the blended-based FRGCs. Whereas the deflection hardening behavior of both slag- and blended-based FRGCs was directly correlated to PE volume content included in the matrix, the ST content showed minor effects on the flexural cracking and ultimate strengths of the FRGCs.
- 4) The mono-PE FRGCs showed a comparative modulus of rupture relative to that of mono-ST FRGCs for both blended- and slag-based composites.
- 5) The use of low content (i.e. 30% by the mass of binder) of 212 μm sand improved the flexural response of both blended- and slag-based FRGCs without violating the deflection hardening conditions.

Acknowledgments

The authors would like to acknowledge the financial support received from the Hong Kong-Guangzhou Technology and Innovation Partnership Programme (Project No.201807010055), National Science Foundation of China (NSFC) Project Nos. 51638008, Innovation Technology Fund (Project code: ITS/009/17) and the Hong Kong Ph.D. Fellowship Scheme (HKPFS) awarded to the first author. Special thanks to the final year students Mr. Ho Sang Lee, Mr. Ka Chun Kong and Mr. Ho Chun Yeung for their precious contribution in conducting the experimental work.

Notations

The following symbols are used in this paper:

DI = ductility index;
 E = composite elastic modulus;
 E_m = matrix elastic modulus;
 f_{cu} = cube compressive strength of composite;
 f_c' = cylinder compressive strength of composite;
 $f_c'm$ = cylinder compressive strength of matrix;
 n = number of cracks;
 S = crack spacing;
 s_{LOP} = flexural cracking strength;
 s_{MOR} = flexural ultimate strength;
 δ_{LOP} = mid-span deflection at cracking load; and
 δ_{MOR} = mid-span deflection at ultimate load.

References

1. T. Matsumoto, H. Mihashi. (2003) "DFRCC terminology and application concepts", *Journal of Advanced Concrete Technology*, 1(3), pp. 335-340.
2. H.-J. Kong, S.G. Bike, V.C. Li. (2003) "Development of a self-consolidating engineered cementitious composite employing electrosteric dispersion/stabilization", *Cement and Concrete Composites* 25(3), (2003), pp. 301-309.
3. K.-Q. Yu, J.-T. Yu, J.-G. Dai, Z.-D. Lu, S.P. Shah, Development of ultra-high performance engineered cementitious composites using polyethylene (PE) fibers, *Construction and Building Materials* 158 (2018) 217-227.
4. S.F.U. Ahmed, H. Mihashi. (2007) "A review on durability properties of strain hardening fibre reinforced cementitious composites (SHFRCC)", *Cement and Concrete Composites*, 29(5), pp. 365-376.
5. M. Maalej, S. Quek, S. Ahmed, J. Zhang, V. Lin, K. Leong. (2012) "Review of potential structural applications of hybrid fiber Engineered Cementitious Composites", *Construction and Building Materials*, 36, pp. 216-227.
6. E.-H. Yang, Y. Yang, V.C. Li. (2007) "Use of high volumes of fly ash to improve ECC mechanical properties and material greenness", *ACI materials journal*, 104(6), 620-628.
7. E. Gartner. (2004) "Industrially interesting approaches to "low-CO₂" cements", *Cement and Concrete research*, 34(9), 1489-1498.
8. F.U.A. Shaikh. (2013) "Review of mechanical properties of short fibre reinforced geopolymer composites", *Construction and Building Materials*, 43, pp. 37-49.
9. T. Alomayri, F. Shaikh, I.M. Low. (2013) "Thermal and mechanical properties of cotton fabric-reinforced geopolymer composites", *Journal of materials science*, 48(19), pp. 6746-6752.
10. M. Alzeer, K. MacKenzie. (2013) "Synthesis and mechanical properties of novel composites of inorganic polymers (geopolymers) with unidirectional natural flax fibres (phormium tenax)", *Applied Clay Science*, 75148-152.
11. T. Lin, D. Jia, P. He, M. Wang, D. Liang. (2008) "Effects of fiber length on mechanical properties and fracture behavior of short carbon fiber reinforced geopolymer matrix composites", *Materials Science and Engineering: A*, 497(1), pp. 181-185.
12. B. Nematollahi, J. Sanjayan, F.U. Ahmed Shaikh. (2015) "Tensile strain hardening behavior of PVA fiber-reinforced engineered geopolymer composite", *Journal of Materials in Civil Engineering*, 27(10), 04015001.
13. B. Nematollahi, J. Sanjayan, J.X.H. Chai, T.M. Lu. (2014) "Properties of fresh and hardened glass fiber reinforced fly ash based geopolymer concrete", *Key Engineering Materials*, Trans Tech Publ, pp. 629-633.
14. K. Vijai, R. Kumutha, B. Vishnuram. (2012) "Effect of inclusion of steel fibres on the properties of geopolymer concrete composites", *Asian journal of civil engineering (building and housing)*, 13(3), pp. 377-85.
15. Z.-h. Zhang, X. Yao, H.-j. Zhu, S.-d. Hua, Y. Chen. (2009) "Preparation and mechanical properties of polypropylene fiber reinforced calcined kaolin-fly ash based geopolymer", *Journal of Central South University of Technology*, 16(1), pp. 49-52.
16. Y. Alrefaei, J.-G. Dai. (2018) "Tensile behavior and microstructure of hybrid fiber ambient cured one-part engineered geopolymer composites", *Construction and Building Materials*, 184, pp. 419-431.
17. M.Z.N. Khan, Y. Hao, H. Hao, F.U.A. Shaikh. (2018) "Mechanical properties of ambient cured high strength hybrid steel and synthetic fibers reinforced geopolymer composites", *Cement and Concrete Composites*, 85, pp. 133-152.
18. F.U.A. Shaikh, A. Fairchild, R. Zammar. (2018) "Comparative strain and deflection hardening behaviour of polyethylene fibre reinforced ambient air and heat cured geopolymer composites", *Construction and Building Materials*, 163, pp. 890-900.
19. F.U.A. Shaikh, A. Patel. (2018) "Flexural Behavior of Hybrid PVA Fiber and AR-Glass Textile Reinforced Geopolymer Composites", *Fibers*, 6(1), pp. 2.
20. M.M. Al-mashhadani, O. Canpolat, Y. Aygörmez, M. Uysal, S. Erdem. (2018) "Mechanical and microstructural characterization of fiber reinforced fly ash based geopolymer composites", *Construction and Building Materials*, 167, pp. 505-513.

21. B. Nematollahi, J. Sanjayan, F.U.A. Shaikh. (2014) "Comparative deflection hardening behavior of short fiber reinforced geopolymer composites", *Construction and Building Materials*, 70, pp. 54-64.
22. F.U.A. Shaikh. (2013) "Deflection hardening behaviour of short fibre reinforced fly ash based geopolymer composites", *Materials & Design*, 50, pp. 674-682.
23. A. Bhutta, P.H.R. Borges, C. Zanotti, M. Farooq, N. Banthia. (2017) "Flexural behavior of geopolymer composites reinforced with steel and polypropylene macro fibers", *Cement and Concrete Composites*, 80, pp. 31-40.
24. P. Sukontasukkul, P. Pongsopha, P. Chindaprasirt, S. Songpiriyakij. (2018) "Flexural performance and toughness of hybrid steel and polypropylene fibre reinforced geopolymer", *Construction and Building Materials*, 161, pp. 37-44.
25. B. Nematollahi, J. Sanjayan, J. Qiu, E.-H. Yang. (2017) "High ductile behavior of a polyethylene fiber-reinforced one-part geopolymer composite: A micromechanics-based investigation", *Archives of Civil and Mechanical Engineering*, 17(3), pp. 555-563.
26. B. Nematollahi, J. Sanjayan, F.U.A. Shaikh. (2016) "Matrix design of strain hardening fiber reinforced engineered geopolymer composite", *Composites Part B: Engineering*, 89, pp. 253-265.
27. Y. Alrefaei, Y.-S. Wang, J.-G. Dai. (2019) "The effectiveness of different superplasticizers in ambient cured one-part alkali activated pastes", *Cement and Concrete Composites*, 97, pp. 166-174.
28. J.L. Provis. (2018) "Alkali-activated materials", *Cement and Concrete Research*, 114, pp. 40-48.
29. Y.-S. Wang, Y. Alrefaei, J.-G. Dai. (2019) "Silico-Aluminophosphate and Alkali-Aluminosilicate Geopolymers: A Comparative Review", *Frontiers in Materials*, 6.
30. T. Luukkonen, Z. Abdollahnejad, J. Yliniemi, P. Kinnunen, M. Illikainen. (2018) "One-part alkali-activated materials: A review", *Cement and Concrete Research*, 103, pp. 21-34.
31. B. Nematollahi, J. Sanjayan, F.U.A. Shaikh. (2015) "Synthesis of heat and ambient cured one-part geopolymer mixes with different grades of sodium silicate", *Ceramics International*, 41(4), pp. 5696-5704.
32. Z. Abdollahnejad, M. Mastali, T. Luukkonen, P. Kinnunen, M. Illikainen. (2018) "Fiber-reinforced one-part alkali-activated slag/ceramic binders", *Ceramics International*, 44(8), pp. 8963-8976.
33. Y. Ling, K. Wang, W. Li, G. Shi, P. Lu. (2019) "Effect of slag on the mechanical properties and bond strength of fly ash-based engineered geopolymer composites", *Composites Part B: Engineering*, 164, pp. 747-757.
34. N.P. Asrani, G. Murali, K. Parthiban, K. Surya, A. Prakash, K. Rathika, U. Chandru. (2019) "A feasibility of enhancing the impact resistance of hybrid fibrous geopolymer composites: Experiments and modelling", *Construction and Building Materials*, 203, pp. 56-68.
35. A. C1018. (1997) "Standard test method for flexural toughness and first crack strength of fiber reinforced concrete (using beam with third point loading)", United States: ASTM Standards.
36. D. joo Kim, A.E. Naaman, S. El-Tawil. (2008) "Comparative flexural behavior of four fiber reinforced cementitious composites", *Cement and concrete Composites*, 30(10), pp. 917-928.
37. Y. Alrefaei, K. Rahal, M. Maalej. (2018) "Shear Strength of Beams Made Using Hybrid Fiber-Engineered Cementitious Composites", *Journal of Structural Engineering*, 144(1), 04017177.
38. J.M. Hodgkinson. (2000) *Mechanical testing of advanced fibre composites*, Elsevier.
39. A. ASTM, (2018) "C39/C39M-18 Standard Test Method for Compressive Strength of Cylindrical Concrete Specimens", ASTM International, West Conshohocken, PA.
40. A. Standard. (2014), "C469/C469M-14, Standard test method for static modulus of elasticity and Poisson's ratio of concrete in compression", ASTM International, West Conshohocken, PA.
41. A. ASTM. (2015) "C617/C617M 15-standard practice for capping cylindrical concrete specimens", ASTM American Society for Testing and Materials-Committee C09 on Concrete and Concrete Aggregates-Subcommittee C, 9.
42. M. Palacios, F. Puertas. (2011) "Effectiveness of Mixing Time on Hardened Properties of Waterglass-Activated Slag Pastes and Mortars", *ACI Materials Journal*, 108(1).
43. J. Shang, J.-G. Dai, T.-J. Zhao, S.-Y. Guo, P. Zhang, B. Mu. (2018) "Alternation of traditional cement mortars using fly ash-based geopolymer mortars modified by slag", *Journal of Cleaner Production*, 203, pp. 746-756.
44. Y. Ding, J.-G. Dai, C.-J. Shi. (2016) "Mechanical properties of alkali-activated concrete: A state-of-the-art review", *Construction and Building Materials*, 127, pp. 68-79.

45. B. Karihaloo, P. Nallathambi. (1990) "Effective crack model for the determination of fracture toughness (KICe) of concrete", *Engineering Fracture Mechanics*, 35(4-5), pp. 637-645.
46. S.F.U. Ahmed, M. Maalej, P. Paramasivam. (2007) "Flexural responses of hybrid steel-polyethylene fiber reinforced cement composites containing high volume fly ash", *Construction and Building Materials*, 21(5), pp. 1088-1097.
47. S. Ahmed, M. Maalej. (2009) "Tensile strain hardening behaviour of hybrid steel-polyethylene fibre reinforced cementitious composites", *Construction and Building Materials*, 23(1), pp. 96-106.
48. V.C. Li, M. Maalej. (1996) "Toughening in cement based composites. Part I: Cement, mortar, and concrete", *Cement and Concrete Composites*, 18(4), pp. 223-237.
49. T. Kanda, V.C. Li. (1999) "New micromechanics design theory for pseudostrain hardening cementitious composite", *Journal of engineering mechanics*, 125(4), pp. 373-381.
50. B. Nematollahi, J. Sanjayan, F. Shaikh. (2015) "Strain hardening behavior of engineered geopolymer composites: effects of the activator combination", *Journal of the Australian ceramics society*, 51(1), pp. 54-60.